(Preprint) AAS 18-16x

IMPULSIVE THRUSTER BASED ATTITUDE STABILITY ANALYSIS OF SPACECRAFT WITH FLEXIBLE SOLAR ARRAYS

Cody Allard[*], Scott Piggott[†] and Hanspeter Schaub[‡]

Stability analysis is an important tool in determining the robustness of the control system design for spacecraft missions. However, many spacecraft exhibit flexible dynamics due to solar arrays or other appended bodies. Therefore, the stability analysis needs to incorporate flexing behavior in the equations of motion. This paper outlines a method for analyzing the stability of spacecraft with flexing solar arrays using classical linear stability analysis techniques such as Bode plots and gain and phase margins. In order to use classical methods for stability analysis, the nonlinear equations that describe the dynamics of spacecraft with flexing solar arrays first need to be linearized. Another aspect to this problem is the equations of motion for the flexing and spacecraft rotation are coupled through second order state variables. This requires the system mass matrix to be inverted to fit the classical state space form. Finally, an eigenvalue diagonalization on the dynamics matrix is necessary to analyze the transfer functions for the stability analysis tools to show the impact of flexing on the performance. This paper summarizes the methods used for the stability analysis and compares the analytical results to numerical results found by simulating a flexible spacecraft using the Basilisk astrodynamics software package. Additionally, the results are compared to rigid body stability analysis results which shows the key influence of flexing on the robustness of the control design.

INTRODUCTION

Many spacecraft have appended solar panels or appended bodies that exhibit flexible behavior. Depending on the characteristics of the appended body, the effects due to this flexible phenomenon sometimes cannot be considered negligible. To quantify the closed-loop attitude pointing performance of these effects, a stability analysis can be performed. This will also show how the control system performs while taking the dynamical effect of flexing solar arrays into consideration.

Stability analysis has extensive history and there are many methods to analyze the stability of a system. When the system is linear, or can be linearized, there are classical techniques used to perform stability analysis which include but are not limited to Bode plots, Nyquist plots, Root Locus plots, and gain and phase margins.[1,2,3] When the system is nonlinear, there are techniques that can used with Lyapunov theory to bound the stability of the system.[2,4] Finally, if the system has multiple inputs and outputs, there are robustness stability analysis techniques such as Nyquist multiple input multiple out stability criteria and h-infinity stability analysis.[5] For this paper, the

[*]Graduate Student, Aerospace Engineering Sciences, University of Colorado Boulder.
[†]ADCS Integrated Simulation Software Lead, Laboratory for Atmospheric and Space Physics, University of Colorado Boulder.
[‡]Professor, Glenn L. Murphy Chair, Department of Aerospace Engineering Sciences, University of Colorado, 431 UCB, Colorado Center for Astrodynamics Research, Boulder, CO 80309-0431. AAS Fellow.

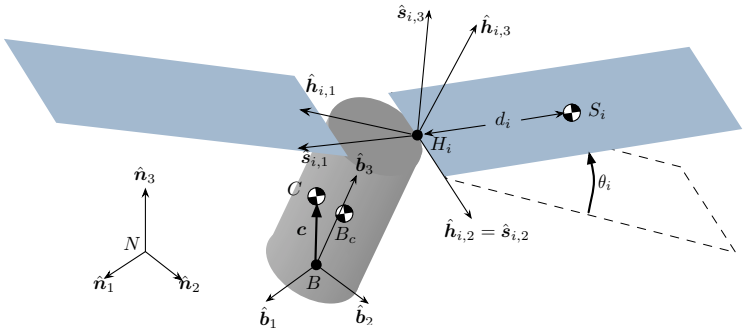

Figure 1. Hinged rigid bodies frame and variable definitions[8]

classical techniques are used because the equations of motion can be linearized well using some assumptions.

One task required to perform a stability analysis is developing the equations of motion that describe the system in consideration. In this case, the unique system under consideration is a spacecraft with flexible solar arrays. One method is to develop the equations of motion considering the appended body as a Bernoulli beam or a continuous flexing structure.[6,7,4] Another method is to assume that the appended body is a rigid body but attached to the spacecraft through a torsional spring.[8] For this paper, the latter method is chosen because of the ease of linearizing the differential equations.

This paper aims to summarize methods that can be used to perform a stability analysis of a spacecraft with flexing solar arrays or appended bodies. The equations of motion are linearized, placed in state space representation, and converted to transfer functions. Then the classical stability analysis tools can be used. This paper is also comparing the linear stability analysis results to the full nonlinear simulation results to show the impact of the linearization process. The following section introduces the equations of motion of a spacecraft with flexing solar arrays.

EQUATIONS OF MOTION

The frame and variable definitions used for the hinged rigid body EOMs development can be seen in Figure 1. Using these definitions, Newtonian/Eulerian mechanics[4,7] and Kane's Method[9,10] were used independently to derive the equations of motion. The equations of motion are introduced in Reference 8 and are repeated here for convenience. The compact, frame independent translational EOM for the hub was found and can be seen in Eq. (1).[8]

$$m_{\text{sc}}\ddot{\boldsymbol{r}}_{B/N} - m_{\text{sc}}[\tilde{\boldsymbol{c}}]\dot{\boldsymbol{\omega}}_{\mathcal{B}/\mathcal{N}} + \sum_{i=1}^{N_s} m_{\text{sp}_i} d_i \hat{\boldsymbol{s}}_{i,3}\ddot{\theta}_i = \boldsymbol{F}_{\text{ext}} - 2m_{\text{sc}}[\tilde{\boldsymbol{\omega}}_{\mathcal{B}/\mathcal{N}}]\boldsymbol{c}' - m_{\text{sc}}[\tilde{\boldsymbol{\omega}}_{\mathcal{B}/\mathcal{N}}][\tilde{\boldsymbol{\omega}}_{\mathcal{B}/\mathcal{N}}]\boldsymbol{c} - \sum_{i=1}^{N_s} m_{\text{sp}_i} d_i \dot{\theta}_i^2 \hat{\boldsymbol{s}}_{i,1} \quad (1)$$

Similarly the hub rotational EOM can be seen in the following equation:[8]

$$m_{\text{sc}}[\tilde{\boldsymbol{c}}]\ddot{\boldsymbol{r}}_{B/N} + [I_{\text{sc},B}]\dot{\boldsymbol{\omega}}_{\mathcal{B}/\mathcal{N}} + \sum_i^{N_s}\left\{ I_{s_i,2}\hat{\boldsymbol{h}}_{i,2} + m_{\text{sp}_i} d_i [\tilde{\boldsymbol{r}}_{S_i/B}]\hat{\boldsymbol{s}}_{i,3} \right\}\ddot{\theta}_i$$
$$= \boldsymbol{L}_B - [\tilde{\boldsymbol{\omega}}_{\mathcal{B}/\mathcal{N}}][I_{\text{sc},B}]\boldsymbol{\omega}_{\mathcal{B}/\mathcal{N}} - [I'_{\text{sc},B}]\boldsymbol{\omega}_{\mathcal{B}/\mathcal{N}} - \sum_i^{N_s}\left\{ \dot{\theta}_i [\tilde{\boldsymbol{\omega}}_{\mathcal{B}/\mathcal{N}}] \left(I_{s_i,2}\hat{\boldsymbol{h}}_{i,2} + m_{\text{sp}_i} d_i [\tilde{\boldsymbol{r}}_{S_i/B}]\hat{\boldsymbol{s}}_{i,3} \right) \right.$$
$$\left. + m_{\text{sp}_i} d_i \dot{\theta}_i^2 [\tilde{\boldsymbol{r}}_{S_i/B}]\hat{\boldsymbol{s}}_{i,1} \right\} \quad (2)$$

Lastly, the hinged rigid body single degree of freedom differential equation can be seen in Eq. (3).[8]

$$m_{\text{sp}_i} d_i \hat{\boldsymbol{s}}_{i,3}^T \ddot{\boldsymbol{r}}_{B/N} + \left[\left(I_{s_i,2} + m_{\text{sp}_i} d_i^2 \right) \hat{\boldsymbol{s}}_{i,2}^T - m_{\text{sp}_i} d_i \hat{\boldsymbol{s}}_{i,3}^T [\tilde{\boldsymbol{r}}_{H_i/B}] \right] \dot{\boldsymbol{\omega}}_{\mathcal{B}/\mathcal{N}}$$
$$+ \left(I_{s_i,2} + m_{\text{sp}_i} d_i^2 \right) \ddot{\theta}_i = -k_i\theta_i - c_i\dot{\theta}_i + \hat{\boldsymbol{s}}_{i,2}^T \boldsymbol{\tau}_{\text{ext},H_i} + \left(I_{s_i,3} - I_{s_i,1} + m_{\text{sp}_i} d_i^2 \right) \omega_{s_i,3}\omega_{s_i,1}$$
$$- m_{\text{sp}_i} d_i \hat{\boldsymbol{s}}_{i,3}^T [\tilde{\boldsymbol{\omega}}_{\mathcal{B}/\mathcal{N}}][\tilde{\boldsymbol{\omega}}_{\mathcal{B}/\mathcal{N}}]\boldsymbol{r}_{H_i/B} \quad (3)$$

Eqs. (1)-(3) provides the 6+N_s EOMs required to describe the motion of the spacecraft with flexing appended bodies. Although these equations are general for N_s number of solar panels, for this paper the number of appended solar panels will be $N_s = 2$. These equations need to be linearized to use classical stability analysis techniques, and this is performed in the following section.

LINEARIZATION

To complete a stability analysis using classical techniques, these equations need to be linearized. One of the first steps of the linearization process is assuming the translational and rotational EOMs are decoupled. Looking at Eqs. (1) and (2), it shows that this coupling comes through the offset vector, $\boldsymbol{c}$, between the body frame origin and the center of mass of the spacecraft. Therefore, throughout the remainder of this work, the body frame origin and the center of mass of the spacecraft will be assumed to be coincident. This is a good assumption when the body frame origin is placed at the equilibrium position of the center of mass of the spacecraft, and when the flexing solar arrays do not change the center of mass location by a substantial amount. For the remainder of this analysis, the cross coupling between the translation and rotational motion is ignored and the translational equation, Eq (1), will not be used. Next, it is assumed that nonlinear and other higher order terms are dropped from the rotational equation:

$$\cancel{m_{\text{sc}}[\tilde{\boldsymbol{c}}]\ddot{\boldsymbol{r}}_{B/N}} + [I_{\text{sc},B}]\dot{\boldsymbol{\omega}}_{\mathcal{B}/\mathcal{N}} + \sum_{i=1}^{N_S}\left\{ I_{s_i,2}\hat{\boldsymbol{s}}_{i,2} + m_{\text{sp}_i} d_i [\tilde{\boldsymbol{r}}_{S_{c,i}/B}]\hat{\boldsymbol{s}}_{i,3} \right\}\ddot{\theta}_i =$$
$$\cancel{-[\tilde{\boldsymbol{\omega}}_{\mathcal{B}/\mathcal{N}}][I_{\text{sc},B}]\boldsymbol{\omega}_{\mathcal{B}/\mathcal{N}}} \cancel{-[I'_{\text{sc},B}]\boldsymbol{\omega}_{\mathcal{B}/\mathcal{N}}} - \sum_{i=1}^{N_S}\left\{ \dot{\theta}_i [\tilde{\boldsymbol{\omega}}_{\mathcal{B}/\mathcal{N}}] \cancel{\left(I_{s_i,2}\hat{\boldsymbol{s}}_{i,2} + m_{\text{sp}_i} d_i [\tilde{\boldsymbol{r}}_{S_{c,i}/B}]\hat{\boldsymbol{s}}_{i,3} \right)} \right.$$
$$\left. \cancel{+ m_{\text{sp}_i} d_i \dot{\theta}_i^2 [\tilde{\boldsymbol{r}}_{S_{c,i}/B}]\hat{\boldsymbol{s}}_{i,1}} \right\} + \boldsymbol{L}_B \quad (4)$$

This simplification results in:

$$[I_{\text{sc},B}]\dot{\boldsymbol{\omega}}_{\mathcal{B}/\mathcal{N}} + \sum_{i=1}^{N_S}\left\{ I_{s_{i,2}}\hat{\boldsymbol{s}}_{i,2} + m_{\text{sp}_i} d_i [\tilde{\boldsymbol{r}}_{S_{c,i}/B}]\hat{\boldsymbol{s}}_{i,3} \right\}\ddot{\theta}_i = \boldsymbol{L}_B \tag{5}$$

Following the same linearization techniques for the flex equation, Eq. (3) simplifies to:

$$\begin{aligned} &m_{\text{sp}_i} d_i \hat{\boldsymbol{s}}_{i,3}^T \ddot{\boldsymbol{r}}_{B/N} + \left[\left(I_{s_{i,2}} + m_{\text{sp}_i} d_i^2 \right) \hat{\boldsymbol{s}}_{i,2}^T - m_{\text{sp}_i} d_i \hat{\boldsymbol{s}}_{i,3}^T [\tilde{\boldsymbol{r}}_{H_i/B}] \right] \dot{\boldsymbol{\omega}}_{\mathcal{B}/\mathcal{N}} + \left(I_{s_{i,2}} + m_{\text{sp}_i} d_i^2 \right) \ddot{\theta}_i \\ &= -k_i\theta_i - c_i\dot{\theta}_i + \hat{\boldsymbol{s}}_{i,2} \cdot \boldsymbol{\tau}_{\text{ext},H_i} + \left(I_{s_{i,3}} - I_{s_{i,1}} + m_{\text{sp}_i} d_i^2 \right) \omega_{s_{i,3}} \omega_{s_{i,1}} - m_{\text{sp}_i} d_i \hat{\boldsymbol{s}}_{i,3}^T [\tilde{\boldsymbol{\omega}}_{\mathcal{B}/\mathcal{N}}][\tilde{\boldsymbol{\omega}}_{\mathcal{B}/\mathcal{N}}] \boldsymbol{r}_{H_i/B} \end{aligned} \tag{6}$$

leading to the following linear relationship:

$$\left[\left(I_{s_{i,2}} + m_{\text{sp}_i} d_i^2 \right) \hat{\boldsymbol{s}}_{i,2}^T - m_{\text{sp}_i} d_i \hat{\boldsymbol{s}}_{i,3}^T [\tilde{\boldsymbol{r}}_{H_i/B}] \right] \dot{\boldsymbol{\omega}}_{\mathcal{B}/\mathcal{N}} + \left(I_{s_{i,2}} + m_{\text{sp}_i} d_i^2 \right) \ddot{\theta}_i = -k_i\theta_i - c_i\dot{\theta}_i \tag{7}$$

In Eq. (7), k_i is the torsional spring constant and c_i is the torsional damping term. Now the nonlinear coupled equations of motion have been linearized to Eqs. (5) and (7) and linear stability analysis techniques can be used.

STATE SPACE REPRESENTATION

A convenient form to place the equations of motion into is a form called state space representation.[1] This form will allow for the classical stability analysis techniques to be used easily while leveraging linear algebra techniques. Since the dynamics are second order differential equations, the associated kinematic differential equations need to be introduced. Modified Rodrigues Parameters (MRPs) are chosen for the attitude parameterization set and the associated MRP differential kinematic equations of motion are given by[4]

$$\dot{\boldsymbol{\sigma}}_{B/N} = \frac{1}{4}[B(\boldsymbol{\sigma}_{B/N})]^{\mathcal{B}}\boldsymbol{\omega}_{B/N} \tag{8}$$

However, these equations also need to be linearized seen in the following equation:

$$\dot{\boldsymbol{\sigma}}_{B/N} = \frac{1}{4}{}^{\mathcal{B}}\boldsymbol{\omega}_{B/N} \tag{9}$$

The linear approximation range for MRPs is with principal rotation up to about 120 degrees. The other kinematic differential equation for the hinged rigid bodies is trivial:

$$\dot{\theta}_i = \frac{\mathrm{d}}{\mathrm{d}t}(\theta_i) \tag{10}$$

To simplify these examples to a two dimensional case, let's assume that the solar array hinge axes are directed along the $\hat{\boldsymbol{b}}_1$ axis, and also assume that spacecraft is constrained to rotate only about the $\hat{\boldsymbol{b}}_1$ axis. Since the equations are linearized and decoupled, the flexing modes only show up in the $\hat{\boldsymbol{b}}_1$ axis so this is a good approximation. Additionally, the equilibrium direction $\hat{\boldsymbol{s}}_1$ for the first solar panel is assumed to be directed along $\hat{\boldsymbol{b}}_2$, and the equilibrium direction $\hat{\boldsymbol{s}}_1$ for the second solar

panel is assumed to be directed along $-\hat{\boldsymbol{b}}_2$. This drastically reduces the complexity of the problem. Now the equations are placed into state space representation and yields the following state vector:

$$\boldsymbol{X} = \begin{bmatrix} \sigma_1 & \omega_1 & \theta_1 & \dot{\theta}_1 & \theta_2 & \dot{\theta}_2 \end{bmatrix}^T \tag{11}$$

where σ_1 is the first MRP coordinate and ω_1 is the first body frame competent of $\boldsymbol{\omega}_{B/N}$. The following state space form is used:[1]

$$[M]\dot{\boldsymbol{X}} = [A]\boldsymbol{X} + [B]\boldsymbol{u} \tag{12}$$

In most cases, the left hand side of the equation is comprised only of the state vector derivative so the following manipulation was completed:

$$\dot{\boldsymbol{X}} = \underbrace{[M]^{-1}[A]}_{[\tilde{A}]}\boldsymbol{X} + \underbrace{[M]^{-1}[B]}_{[\tilde{B}]}\boldsymbol{u} \tag{13}$$

Eqs. (5), (7), (9), and (10) are converted into the state space representation matrices beginning with matrix $[M]$:

$$\begin{bmatrix} 1 & 0 & 0 & 0 & 0 & 0 \\ 0 & I_{11} & 0 & -I_{sp,2} - m_{sp}dd_{S_c/B} & 0 & I_{sp,2} + m_{sp}dd_{S_c/B} \\ 0 & 0 & 1 & 0 & 0 & 0 \\ 0 & -(I_{sp,2} + m_{sp}d^2) - m_{sp}dd_{H/B} & 0 & I_{sp,2} + m_{sp}d^2 & 0 & 0 \\ 0 & 0 & 0 & 0 & 1 & 0 \\ 0 & (I_{sp,2} + m_{sp}d^2) + m_{sp}dd_{H/B} & 0 & 0 & 0 & I_{sp,2} + m_{sp}d^2 \end{bmatrix} \tag{14}$$

where $I_{sp,2}$ is the inertia of the solar panel about its second solar panel axis seen in Figure 1, I_{11} is the inertia of the rigid body hub about the first body axis, $d_{S_c/B}$ is the distance between the body frame origin and the solar panels center of mass, and $d_{H/B}$ is the distance between the body frame origin and the hinge location. Next, matrices $[A]$, $[B]$ and $\boldsymbol{u}$ are defined:

$$[A] = \begin{bmatrix} 0 & 0.25 & 0 & 0 & 0 & 0 \\ 0 & 0 & 0 & 0 & 0 & 0 \\ 0 & 0 & 0 & 1 & 0 & 0 \\ 0 & 0 & -k & -c & 0 & 0 \\ 0 & 0 & 0 & 0 & 1 & 0 \\ 0 & 0 & 0 & 0 & -k & -c \end{bmatrix} \tag{15}$$

$$[B] = \begin{bmatrix} 0 & 1 & 0 & 0 & 0 & 0 \end{bmatrix}^T \tag{16}$$

$$\boldsymbol{u} = [\tau_1] \tag{17}$$

where τ_1 is the control torque applied about the first body frame axis, $\hat{\boldsymbol{b}}_1$.

Next, the output equation is defined in the following equation:

$$\boldsymbol{Y} = [C]\boldsymbol{X} + [D]\boldsymbol{u} = \begin{bmatrix} \sigma_1 & \omega_1 & \theta_1 & \dot{\theta}_1 & \theta_2 & \dot{\theta}_2 \end{bmatrix}^T \tag{18}$$

with $[C]$ and $[D]$ defined as

$$[C] = \begin{bmatrix} 1 & 0 & 0 & 0 & 0 & 0 \\ 0 & 1 & 0 & 0 & 0 & 0 \\ 0 & 0 & 1 & 0 & 0 & 0 \\ 0 & 0 & 0 & 1 & 0 & 0 \\ 0 & 0 & 0 & 0 & 1 & 0 \\ 0 & 0 & 0 & 0 & 0 & 1 \end{bmatrix} \tag{19}$$

$$[D] = \begin{bmatrix} 0 & 0 & 0 & 0 & 0 & 0 \end{bmatrix}^T \tag{20}$$

The output equation is meant to include all of the outputs so that when the equations are converted to transfer functions, eigenvalues can be computed on the resulting matrices.

It should be noted that the matrices included above are the continuous time representation of the system. The system can be converted to a discrete time representation by either using a software package or the analytical conversion. This conversion is not discussed in this document.

Now that the state space representation has been defined (the open loop portion), the closed loop definition of this problem is defined in the next section.

CLOSED LOOP STATE SPACE REPRESENTATION

First, the feedback definition for the control in the state space form is defined in the following equation.[1]

$$\boldsymbol{u} = -[K](\boldsymbol{X} - \boldsymbol{X}_{\text{ref}}) = \tau_1 \tag{21}$$

Where $[K]$ is the gain matrix. The gain matrix chosen for this paper is:[4]

$$[K] = \begin{bmatrix} K_1 P - 0.25 K_1^2 I_{11} & P & 0 & 0 & 0 & 0 \end{bmatrix} \tag{22}$$

If there is an integral term for σ_1, then the gain that is associated with $\int \sigma_1$ is $K_I K_1$. This addition can easily be applied to the state space representation since the time derivative of $\int \sigma$ is σ.

Finally, to complete the closed loop state space representation, the following equations are needed:

$$\dot{\boldsymbol{X}} = [M]^{-1}[A]\boldsymbol{X} - [M]^{-1}[B][K]\boldsymbol{X} + [B][K]\boldsymbol{X}_{\text{ref}} \tag{23}$$

$$\dot{\boldsymbol{X}} = [M]^{-1}\Big([A] - [B][K]\Big)\boldsymbol{X} + [B][K]\boldsymbol{X}_{\text{ref}} \tag{24}$$

The state space representation for both the open loop and closed loop systems are useful for simulating the linear response, and converting to the frequency domain space for completing a phase and gain margin analysis. The following section will summarize the techniques used for converting the between state space and the frequency domain.

STATE SPACE TO TRANSFER FUNCTION CONVERSION

The following equation is used to convert from the time domain to the frequency domain:

$$[G(s)] = [C]\Big(s[I] - [A]\Big)[B] \tag{25}$$

Where $[G(s)]$ is the transfer function matrix and s is the frequency. where each element corresponds the transfer function that relates an input to an output. This method can be used to find both the open loop and closed loop transfer function matrices using the corresponding $[A]$ and $[B]$ matrices, depending on which form.

However, another way to convert from the time domain to the frequency domain is to use the following two equations:

$$[G(s)]_{OL} = [C]\Big(s[I] - [A]\Big)[B][K] \tag{26}$$

$$[G(s)]_{CL} = \frac{[G(s)]_{OL}}{I + [G(s)]_{OL}} \tag{27}$$

Where the subscripts OL and CL are corresponding to open loop and closed loop respectively. Now all of the equations of motion have been developed to perform a phase and gain analysis on the system.

RESULTS

This section uses the stability analysis tools on specific examples to highlight the effects of flexing solar arrays on the stability of the spacecraft. The following table summarizes the physical parameters used for the results in this section. There are two solar panels attached to the spacecraft and they have the same physical parameters seen in Table 1.

Table 1. Spacecraft parameters

Name	Description	Value	Units
I_{11}	Rigid body hub inertia about $\hat{\boldsymbol{b}}_1$ axis	500.0	kg-m^2
$I_{sp,2}$	Inertia of solar panel about $\hat{\boldsymbol{s}}_2$ axis	100	kg-m^2
m_{sp}	mass of solar panel	30	kg
d	distance from hinge location to CoM of solar panel	1.5	m
$d_{H/B}$	distance from body frame location to hinge location	1	m
$d_{S_c/B}$	distance from body frame location to CoM of solar panel	1	m
k	spring constant	1200	N-m/rad
c	damping constant	9	N-m-s/rad

Open Loop Stability Analysis Results

In general, an uncontrolled spacecraft is typically considered marginally stable, unless there is some form of passive stability like gravity gradient. In our case, the spacecraft can be assumed to be marginally stable, meaning that the dynamics matrix has values of zero for the pole locations and if the system is perturbed by a step response, the spacecraft will just drift at a constant angular speed.

For this open loop stability analysis, a bode plot is created for three different control gains. These three scenarios are used to show the performance and robustness of the control system with different gains.

The control gains used for each scenario is summarized in Table 2. Figures 2-4 show the results from the bode plots for the open loop system for each set of control gains. These are the discrete-time systems - with the control frequency set to 2 Hz. The open loop bode plot is useful because it gives insight into how much the system is close to an instability region. Quantitatively, these values are the gain and phase margins. Using the open loop bode plots the gain and phase margin for each

Table 2. Gain Descriptions for the three scenarios

Scenario	K_1	K_I	P
Scenario 1	0.15	0.0	100
Scenario 2	0.5	0.0	600
Scenario 3	3	25	175

mode was found and can be seen Table 3. It should be noted that both the rigid body response and the flexible response is plotted on the bode plots. The green curve is the flexible system response, and blue curve is the rigid body response. There is good agreement between the rigid body and flexible system response at most all frequencies except for close to the frequency of the solar arrays. The solar arrays first mode frequency is at 0.9 Hz, and there is a noticeable difference between the rigid body and flexible system response. However, from the open loop analysis, this does not greatly impact performance.

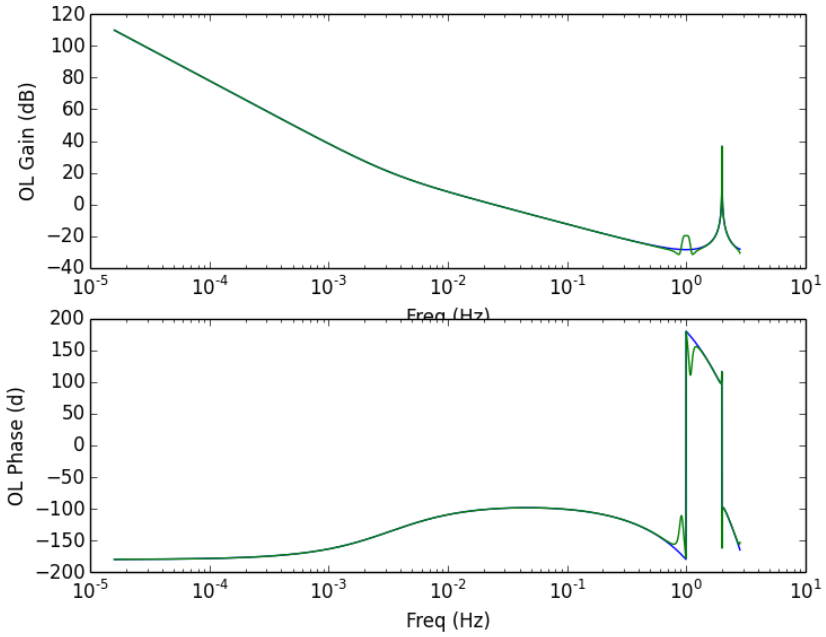

Figure 2. Open loop bode plot for Scenario 1 gains (blue is rigid response, green is flexible body response)

Table 3. Gain Descriptions for Analyzed Operaton Modes

Scenario	Gain (db)	Phase (deg)
Safe Mode	28	81
RWA	12	72
DV	2.8	153

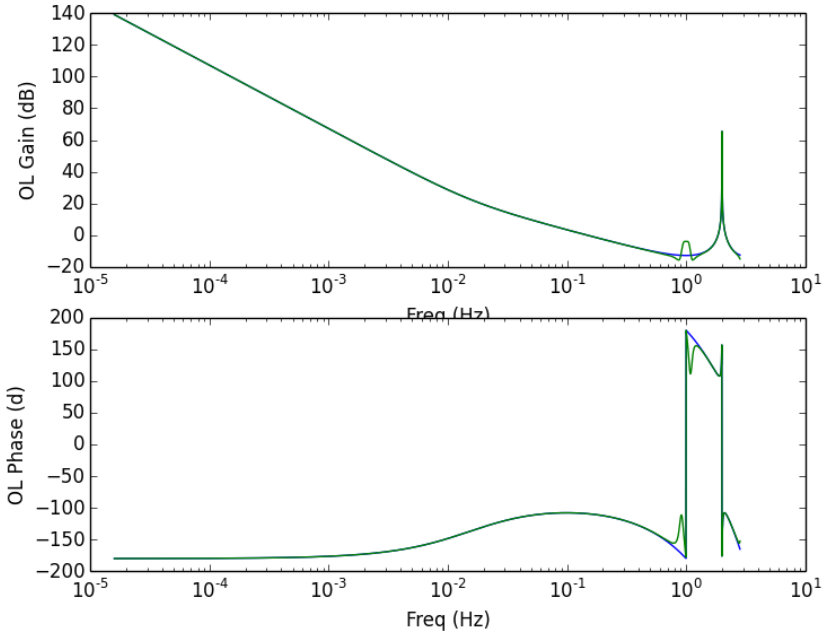

Figure 3. Open loop bode plot for Scenario 2 gains

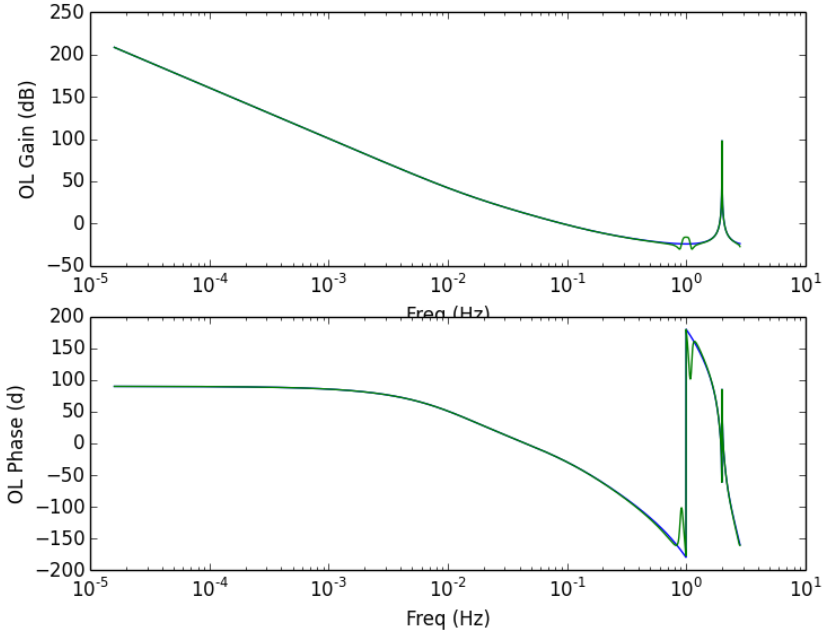

Figure 4. Open loop bode plot for Scenario 3 gains

Closed Loop Stability Analysis Results

The closed loop stability analysis is useful for looking at the closed loop performance, the steady state response of the system, and how well the system will track a frequency response over a frequency range. This is particularly useful in systems like this one that are marginally stable, because the system will always be closed loop to elicit the desired control response. Using the analytical development for converting the open loop to a closed loop system and converting the continuous time state space model to the frequency a bode plot analysis was performed. A bode plot was created for each set of control gains. The results from this analysis can be seen in Figures 5- 7. It should be noted that again the rigid body response curve is in blue, and the green curve is flexible body response. Additionally, simulation results using the Basilisk astrodynamics software package can seen in Figs. 5- 7 labeled with the red hash marks. The Basilisk simulation results use the full nonlinear equations of motion. The reason for doing this is to show the agreement between the analytical frequency domain response using the linearized equations and the numerical results from the full nonlinear equations simulation.

The results show that the system tracks very well at low frequencies and at high frequencies the performance degrades but the system does not go unstable. Additionally, the numerical simulation agrees well with the analytical development, and the flexible dynamics better models the system response than the rigid body response. The spikes in the bode plots that are near the solar array frequency (0.9 Hz) and the Nyquist frequency (1 Hz) are due to the flexible dynamics and the degradation of performance while nearing a Nyquist frequency. Further analysis will be completed in this region, and to see why there is some disagreement between the numerical simulation and the analytical frequency response at these frequencies. However, the results are promising and give confidence in the control gains selected.

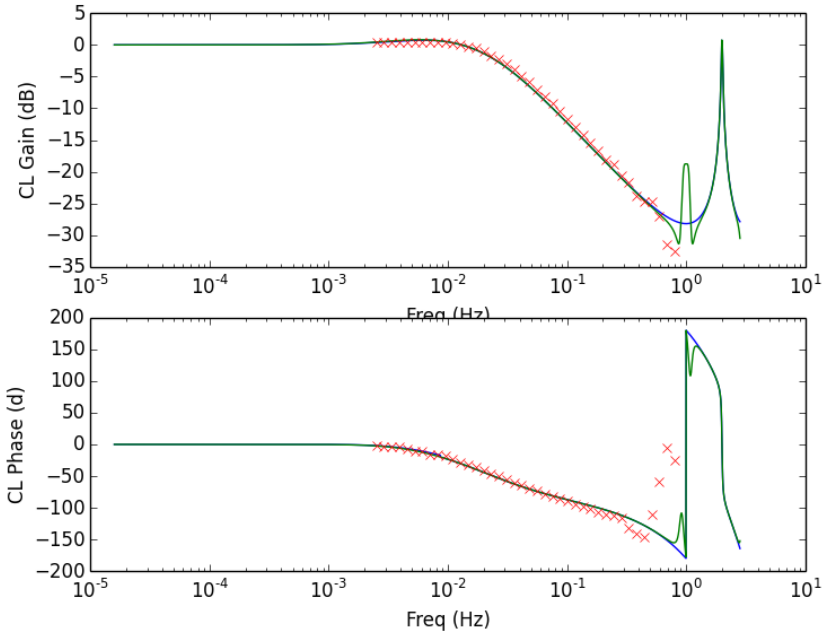

Figure 5. Closed loop bode plot for Scenario 1 gains

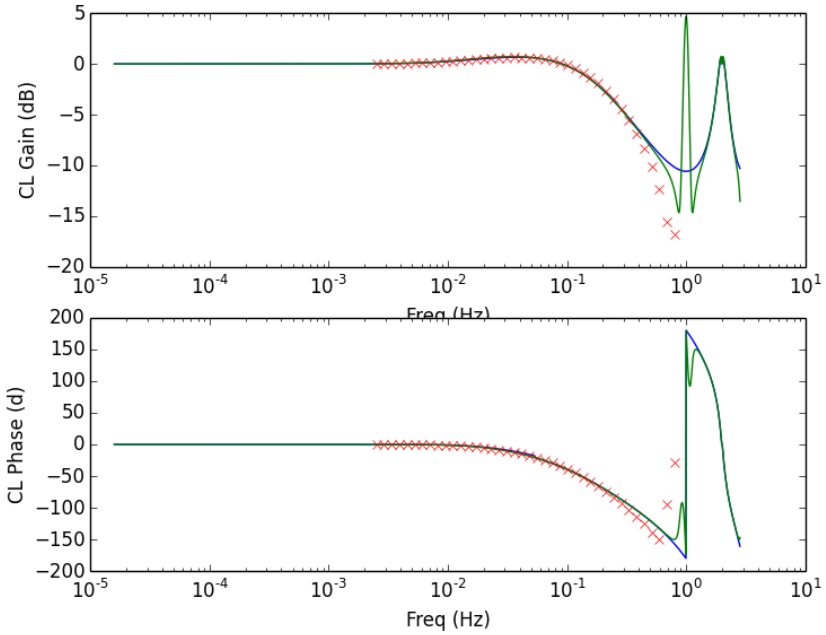

Figure 6. Closed loop bode plot for Scenario 2 gains

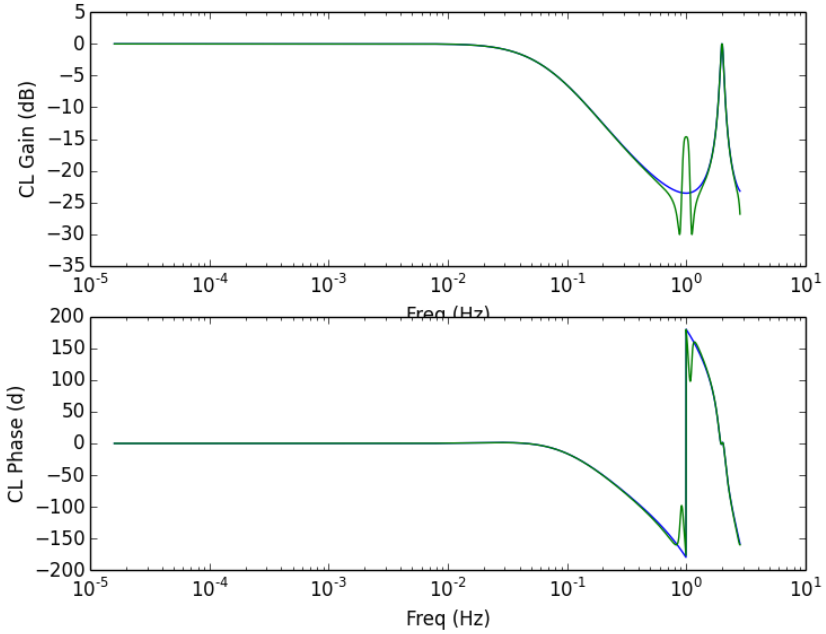

Figure 7. Closed loop bode plot for Scenario 3 gains

CONCLUSION

This paper summarizes some analytical tools that can be used to perform stability analysis of spacecraft with flexing solar arrays using classical methods like Bode plot and gain and phase mar-

gins. The stability analysis results include a comparison between rigid body stability analysis and the proposed method. The results highlight the difference between the two and show why this can be important to include in stability studies. Additionally, the linearized stability analysis is compared to the full non-linear equations of motion stability results and these show good agreement. However, there is some disagreement as the results got closer to the solar array frequency and the Nyquist frequency. Further investigation needs to be completed to fully quantify the reason for this discrepancy.

REFERENCES

[1] C. Kluever, *Dynamic Systems: Modeling, Simulation, and Control*. Wiley, 2015.

[2] K. Åström and R. Murray, "Feedback Systems: An Introduction for Scientists and Engineers," 01 2008.

[3] B. Friedland, *Control system design: an introduction to state-space methods*. McGraw-Hill series in electrical engineering: Control theory, McGraw-Hill, 1986.

[4] H. Schaub and J. L. Junkins, *Analytical Mechanics of Space Systems*. Reston, VA: AIAA Education Series, 3rd ed., 2014, 10.2514/4.102400.

[5] S. Skogestad and I. Postlethwaite, *Multivariable Feedback Control: Analysis and Design*. Wiley, 2005.

[6] J. L. Junkins and Y. Kim, *Introduction to Dynamics and Control of Flexible Structures*. Washington D.C.: AIAA Education Series, 1993.

[7] M. Sidi, *Spacecraft Dynamics and Control: A Practical Engineering Approach*. Cambridge Aerospace Series, Cambridge University Press, 1997, 10.1017/CBO9780511815652.

[8] C. Allard, H. Schaub, and S. Piggott, "General Hinged Solar Panel Dynamics Approximating First-Order Spacecraft Flexing," *AAS Guidance and Control Conference*, Breckenridge, CO, Feb. 5–10 2016. Paper No. AAS-16-156.

[9] T. R. Kane, P. W. Likins, and D. A. Levinson, *Spacecraft dynamics*. McGraw-Hill Book Co., 1983.

[10] T. R. Kane and D. A. Levinson, "Formulation of Equations of Motion for Complex Spacecraft," *Journal of Guidance, Control, and Dynamics*, Vol. 3, 2017/09/27 1980, pp. 99–112, 10.2514/3.55956.